Preparation of a Nanosilica-Modified Negative-Type Acrylate Photoresist

Dar-Jong Lin, Trong-Ming Don, Chin-Chung Chen, Bing-Yi Lin, Chih-Kang Lee, Liao-Ping Cheng

Department of Chemical and Materials Engineering, Tamkang University, Taipei, Taiwan 25137

Received 13 March 2007; accepted 26 June 2007
DOI 10.1002/app.27151
Published online 9 October 2007 in Wiley InterScience (www.interscience.wiley.com).

ABSTRACT: A new type of negative photoresist, which incorporated nanosized silica into a photosensitive acrylic resin, was developed. First, free-radical polymerization was employed to synthesize the acrylic resin, poly[methyl methacrylate/methacrylic acid/3-(trimethoxysilyl) propyl methacrylate], and then a silica precursor, prepared by hydrolysis and condensation of tetraethoxysilane in a sol–gel process, was introduced into the as-formed resin solution. After the addition of photosensitive monomers and photoinitiators, a negative-type organic–inorganic photoresist was produced. The morphology of the UV-cured photoresist, as observed by field emission scanning electron microscopy, indicated that the size of the silica domain in the material could be reduced from 300 to about 50 nm by appropriate dosage of 3-(trimethoxysilyl) propyl methacrylate. Thermogravimetric analysis, dynamic mechanical analysis, differential scanning calorimetry, and thermal mechanical analysis were used to evaluate the thermal and dimensional stabilities of the cured photoresists. It was found that the thermal decomposition temperature and glass-transition temperature increased, whereas the thermal expansion coefficients before and after the glass transition decreased, with increasing silica content. The incorporation of 3-(trimethoxysilyl) propyl methacrylate also enhanced the thermal and dimensional stabilities; however, the level of enhancement was moderate for the thermal decomposition temperature and thermal expansion coefficient and low for the glass-transition temperature. In addition, a photoresist coated on a copper substrate demonstrated high hardness (5H) and strong adhesion (100%) with a resolution of 30 μm. © 2007 Wiley Periodicals, Inc. J Appl Polym Sci 107: 1179–1188, 2008

Key words: composites; photoresists; silicas

INTRODUCTION

Photosensitive organic–inorganic nanocomposites have widely been investigated for both scientific and application purposes.[1–5] Organic polymers with specific physical properties, such as good flexibility, ductility, and processability, have long been extensively applied in various fields. On the other hand, inorganic materials possess different yet complementary properties, such as high rigidity, mechanical strength, and thermal stability. The combination of the advantages offered by these two classes of materials to yield a composite with superior properties that meet industrial standards is highly demanded. Although conventional organic–inorganic blends usually suffer from the large micrometer-scale phase-separation problem, the incorporation of the inorganic component in the form of uniformly dispersed nanoparticles into a continuous polymer matrix has been demonstrated to be a promising route.[6–11]

The sol–gel process is a method widely used to prepare organic–inorganic hybrid materials. Originally, this process was developed for the low-temperature synthesis of glass or ceramic materials. In general terms, the process involves consecutive hydrolysis and condensation of an alkoxysilane to form silicone oxides that are suspended in an aqueous/alcohol solution; for example, silica can be formed through the hydrolysis and condensation of tetraethoxysilane (TEOS). The related theories were built on colloidal science, and the basic principles can be found in previous literature.[12,13] If an organic material such as a polymer is introduced into the sol–gel process, organic–inorganic composite materials can be produced. The key to success in forming polymer–inorganic composites by the sol–gel process lies in the fact that the reactions can be carried out at temperatures common to polymer synthesis in an appropriate solvent. It has been reported that under proper preparation conditions, the dimensions of the particles in the formed composite can be brought down to the level of 1–20 nm.[9,12] Therefore, the composite material is optically transparent and is thus suited to optoelectronic applications.[14–16]

In this research, organic–inorganic composite materials were synthesized by means of a modified sol–gel process. The inorganic moieties, that is, silica particles, were covalently bonded and uniformly

Correspondence to: L.-P. Cheng (lpcheng@mail.tku.edu.tw).

Journal of Applied Polymer Science, Vol. 107, 1179–1188 (2008)
© 2007 Wiley Periodicals, Inc.

WILEY InterScience® DISCOVER SOMETHING GREAT

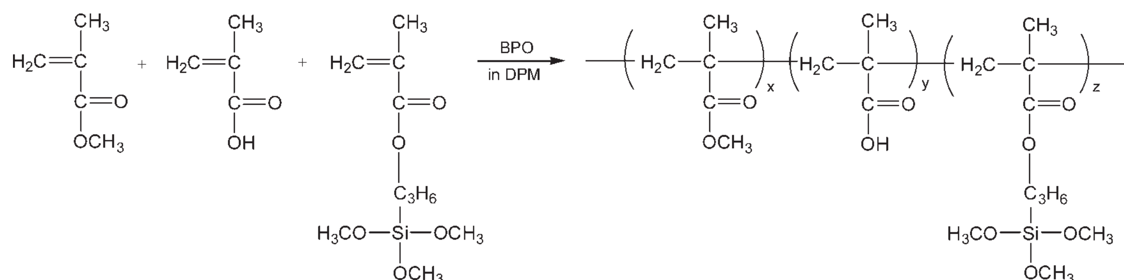

Scheme 1

dispersed in the organic polymer matrix, which consisted of methyl methacrylate (MMA), methacrylic acid (MAA), and/or 3-(trimethoxysilyl) propyl methacrylate (MSMA) monomeric repeating units. The synthesis routes are outlined in Schemes 1 and 2 Polyacrylate was prepared by free-radical copolymerization of the three kinds of acrylic monomers at an elevated temperature. The coupling agent, MSMA, in the formed copolymer was then reacted with silica sol that was prepared separately by a normal sol–gel process from TEOS.[17–19] The incorporation of the coupling agent enhanced the compatibility between inorganic and organic components, and this gave rise to interesting morphological features and improved thermal mechanical properties. Furthermore, a negative-type photoresist was prepared by the addition of photoinitiators and crosslinking agents to the formed polyacrylate/silica solution. With a standard UV-exposure process, a cured photoresist was obtained. Its properties, such as the thermal and dimensional stability, mechanical strength, adhesion, and resolution, were determined and compared to examine the effects of silica and MSMA.

EXPERIMENTAL

Materials

Materials for the preparation of polyacrylate/silica composites, including MMA, MAA, MSMA, TEOS, benzoyl peroxide (BPO), and dipropylene glycol monomethyl ether (DPM), were reagent-grade and were purchased from Aldrich Chemical Co. (Milwaukee, WI). Crosslinking agents for producing photoresists, dipentaethritol hexaacrylate (DPHA) and trimethylol propane triacrylate (TMPTA), were also purchased from Aldrich Chemical. Photoinitiators 2-methyl-1-[4-(methylthio)phenyl]-2-morpholinopropanone-1 (Irgacure 907) and isopropyl thioxanthone (ITX) were supplied by Ciba–Geigy, Ltd. (Tarrytown, NY). All materials were used as received.

Preparation of the methacrylate polymer

Acrylic ester copolymers were prepared by free-radical copolymerization of monomers MMA, MAA, and/or MSMA (cf. Scheme 1). Appropriate amounts of these monomers were dissolved in DPM. The solution was heated to 90°C under a nitrogen atmosphere. Initiator BPO (1 wt % of the monomers), previously dissolved in DPM, was added to the solution, and the polymerization reaction was carried out for 6 h. The obtained polymer solution (termed the polyacrylate solution hereafter) was cooled to room temperature and diluted with tetrahydrofuran. The diluted solution was poured into hexane to induce polymer precipitation. The polymer was separated by filtration and was dried *in vacuo* at 60°C. The precipitation procedure was repeated twice to ensure that it was free of the residual monomers. The compositions of various copolymers are listed in Table I.

Preparation of the silica–polyacrylate composite and photoresist

The silica sol was prepared by the hydrolysis and condensation of TEOS in deionized water at room temperature. The H_2O/TEOS molar ratio was 2, and a nitric acid aqueous solution at pH 1.1 was used as a catalyst. The reaction was allowed to proceed for 2 h, and then the formed silica sol was added to the as-prepared polyacrylate solution at room temperature. After another hour of reaction, the polyacrylate/SiO_2 composite material was obtained (cf.

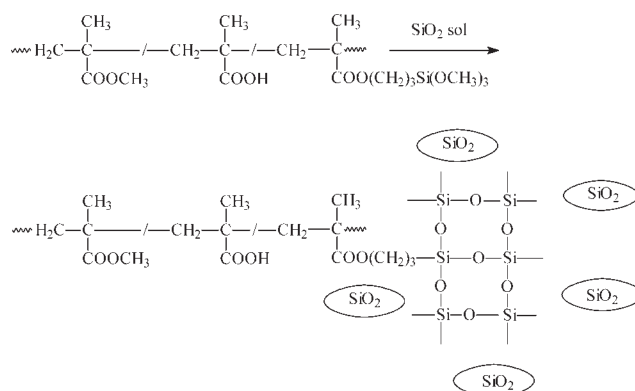

Scheme 2

TABLE I
Compositions of the Polyacrylate/SiO_2 Hybrid Materials

Sample name	Weight ratio of the monomers (MMA : MAA : MSMA)	SiO_2 content (wt %)
B1M0-0	3.5 : 1 : —	0
B1M0-8	3.5 : 1 : —	8
B1M0-14	3.5 : 1 : —	14
B1M0-21	3.5 : 1 : —	21
B1M1-0	3.5 : 1 : 0.045	0
B1M1-8	3.5 : 1 : 0.045	8
B1M1-14	3.5 : 1 : 0.045	14
B1M1-21	3.5 : 1 : 0.045	21
B1M3-0	3.5 : 1 : 0.135	0
B1M3-8	3.5 : 1 : 0.135	8
B1M3-14	3.5 : 1 : 0.135	14
B1M3-21	3.5 : 1 : 0.135	21
B1M5-0	3.5 : 1 : 0.225	0
B1M5-8	3.5 : 1 : 0.225	8
B1M5-14	3.5 : 1 : 0.225	14
B1M5-21	3.5 : 1 : 0.225	21
B1M7-0	3.5 : 1 : 0.314	0
B1M7-8	3.5 : 1 : 0.314	8
B1M7-14	3.5 : 1 : 0.314	14
B1M7-21	3.5 : 1 : 0.314	21

Scheme 2). The compositions of the silica and polymer can be found in Table I.

Subsequently, negative acrylate photoresists were prepared by the addition of suitable amounts of photoinitiators (Irgacure 907/ITX = 4) and crosslinking agents DPHA (10 wt % of the photoresist) and TMPTA (10 wt % of the photoresist). These photoresists were uniformly spread on a poly(ethylene terephthalate) substrate with a casting knife (100 μm) and then predried at 80°C for 50 min; this was followed by UV irradiation at 80 mJ/cm^2 to obtain cured films. Monolith samples were also prepared for thermal analysis. The photoresist was poured into a Teflon mold and then cured with the same procedure.

Characterization

Several methods were adopted to characterize the composite material and the photoresist:

1. Infrared absorption spectra of the photoresist before and after UV curing were taken with a Fourier transform infrared (FTIR) spectrophotometer (model 550, Nicolet, Madison, WI). Uncured samples were prepared by appropriate amounts of the photoresist being dropped onto a KBr disc, and then the solvent was evaporated at 80°C. After FTIR scans were taken, the sample was UV-cured and then scanned again. For both scans, the spectra were collected over the wave-number range of 400–4000 cm^{-1} with a resolution of 4 cm^{-1}.
2. Thermogravimetric analysis (TGA; Hi-Res TGA 2950, TA Instruments, Ltd., New Castle, DE) was used to measure the thermal decomposition temperature (T_d) of the photoresist films. Samples (8–12 mg) were heated from room temperature to 600°C with a scanning rate of 10°C/min under a nitrogen flow.
3. Differential scanning calorimetry (DSC) and dynamic mechanical analysis (DMA) were both employed to measure the glass-transition temperature (T_g) of the prepared films. DSC (model DSC 200, Netzsch Corp., Mohnopumpen GmbH) was first calibrated with an indium standard before the tests were run. An appropriate amount of a dried sample was sealed in an aluminum pan and placed in the heating chamber together with an empty reference pan. The temperature was raised from 50 to 180°C at a constant rate of 10°C/min under a nitrogen flow. T_g of the sample was determined from the thermogram of the second heating cycle. Dynamic mechanical properties were measured with DMA (model DMA Q800, TA Instruments). Experiments were carried out on dried samples with a frequency of 1 Hz and at a heating rate of 5°C/min. To compare the T_g obtained from mechanical damping (tan δ) with that from DSC (heat capacity), the DMA spectra of the second heating cycle from 50 to 180°C were analyzed. All samples were 22.4 mm long between clips, 5.0 mm wide, and about 1 mm thick.
4. The thermal expansion behaviors of the cured films were studied with thermal mechanical analysis (TMA; model TMA Q400, TA Instruments). The thermal expansion coefficients before and after the glass transition (α_1 and α_2, respectively) were obtained by the measurement of the linear dimensional variations (ΔL) at different temperatures. The T_g of a sample was identified as the intercept of the two tangent lines at which a change in slope occurred, that is, above and below T_g. The samples (4 mm × 8 mm) were heated from 30 to 180°C with a scanning rate of 10°C/min in a nitrogen atmosphere.
5. The nanoscale morphology of the silica sol and the formed films was observed with transmission electron microscopy (TEM) and field emission scanning electron microscopy (FESEM), respectively. TEM images were taken with a JEOL (Tokyo, Japan) JEM-1200EXII. TEM sampling grids were prepared by 2 μg of the silica sol being dropped onto a standard copper grid, and the solution was evaporated at room temperature. On the other hand, the cross-sectional morphologies of the formed films were observed with FESEM (Leo 1530, Carl Zeiss, Oberkochen,

Germany). The samples were vacuum-dried and then fractured in liquid nitrogen to expose the cross sections. The lateral sides of the samples were wrapped with conductive copper tape and clamped in a cross-section sample holder. They were then coated with a thin layer (ca. 3.0 nm) of a Pt–Pd alloy and observed under 2–10-kV acceleration voltages with an in-lens detector.

6. Tape tests, also called peel tests, were carried out to evaluate the adhesion of the films coated on a copper substrate. The degree of adhesion between the films and copper sheets increased as the percentage of the residual film after the tape test increased.[20] The hardness of the formed films was examined by the industrial pencil hardness test with pencils of different hardness.[21]

RESULTS AND DISCUSSION

FTIR analysis

The evolution of chemical bonds during the sol–gel and UV-curing processes was observed with FTIR. In Figure 1, the spectra of pure TEOS and silica obtained by a sol–gel process are presented. For the silica sample, the adsorption bands at 1072 and 796 cm^{-1} represent the asymmetric and symmetric stretching vibrations of the Si—O—Si bond, respectively. The 453-cm^{-1} band is the bending vibration of this bond. The bands for —Si—O—C— and Si—OH stretching vibrations are located at 1100 and 3348 cm^{-1}, respectively. The adsorption band at 940 cm^{-1} is assigned to the Si—OH bond. By comparison with the spectrum of TEOS, the hydrolysis and condensation of TEOS to produce silica can be confirmed.[22] Figure 2 shows the FTIR spectra of the synthesized poly(methyl methacrylate/methacrylic acid) [poly(MMA/MAA)] and poly[methyl methacrylate/methacrylic acid/3-(trimethoxysilyl) propyl methacrylate] [poly(MMA/MAA/MSMA)]. The bands at 3400–3600 cm^{-1} for —OH stretching, at 1732 cm^{-1} for C=O stretching, and at 2994 cm^{-1} for —CH_3 stretching are in evidence. After we bring the two spectra close together in Figure 3, it becomes simple to distinguish these two polymers. The band standing for the —Si—O—C— stretching vibration of MSMA can be found at 1089 cm^{-1}. Figure 4 shows the FTIR spectra of a typical polyacrylate/SiO_2 photoresist before and after it was UV-cured. It can be seen that the C=C stretching band at 1634 cm^{-1} decreases considerably after the irradiation process. In other words, the curing process has effectively converted the multifunctional monomers, TMPTA and DPHA, into a crosslinked network structure.

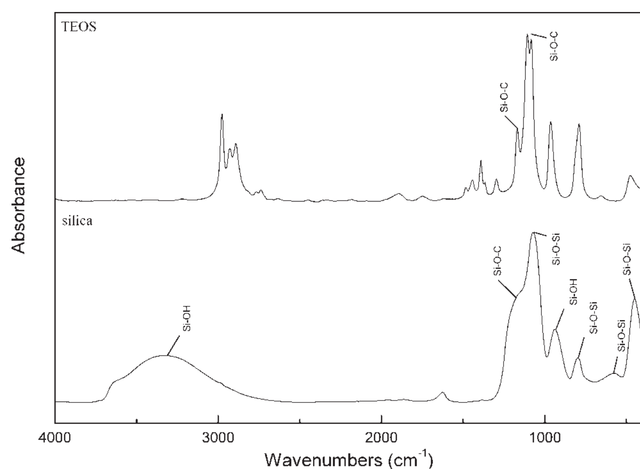

Figure 1 FTIR spectra of pure TEOS and silica.

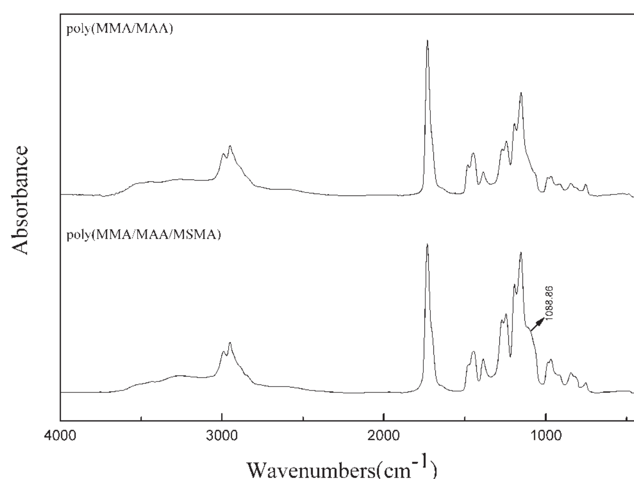

Figure 2 FTIR spectra of poly(MMA/MAA) (i.e., B1M0-0) and poly(MMA/MAA/MSMA) (i.e., B1M1-0).

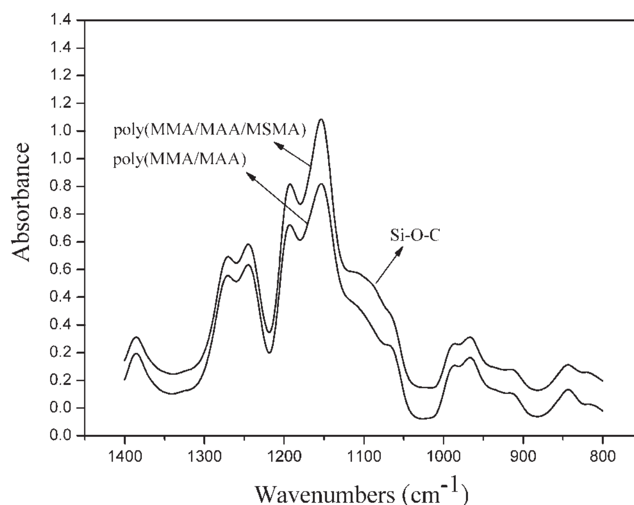

Figure 3 FTIR spectra of poly(MMA/MAA) and poly (MMA/MAA/MSMA) in the wave-number range of 800–1400 cm^{-1}.

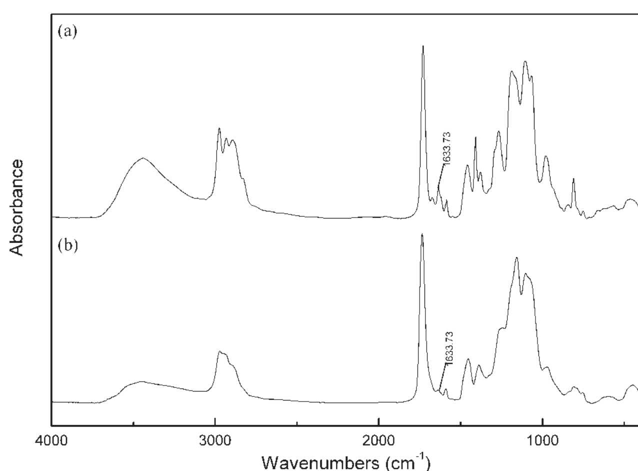

Figure 4 FTIR spectra of the negative acrylate photoresist (B1M1-8) (a) before and (b) after UV curing.

Nanoscale morphology

The sizes of the silica particles in the sol prepared by hydrolysis and condensation of TEOS were observed with TEM. Figure 5 shows an image of several isolated particles (black dots). The average size of the particles has been measured to be about 40 nm. Some large clusters (e.g., 60 nm), considered to arise from aggregation of small particles, can also be observed. Photoresists with different silica and MSMA contents were prepared, and their nanoscale fine structures were observed with FESEM. Figure 6 shows the images of three representative cases: B1M0-0, B1M0-8, and B1M3-8. For the plain photoresist, B1M0-0, free of coupling agent and silica, Figure 6(a) demonstrates a dense and uniform cross-sectional morphology. The particulate entities, some tens of nanometers in size, are the sputtered grains of the Au–Pt alloy. As silica was incorporated without

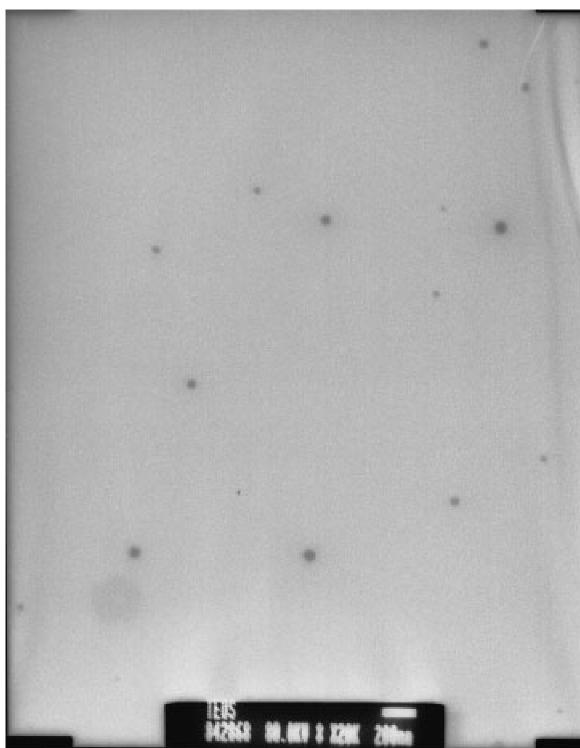

Figure 5 TEM image of silica particles in the sol (20,000×).

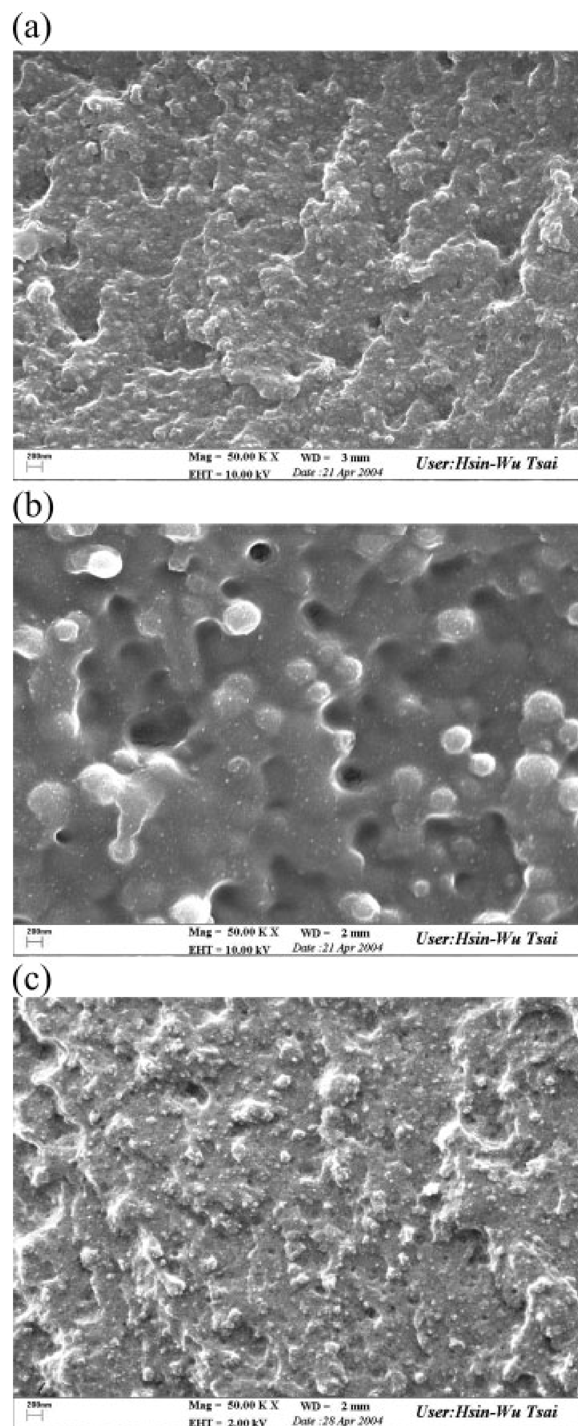

Figure 6 SEM micrographs of the cross sections of UV-cured photoresists: (a) B1M0-0, (b) B1M0-8, and (c) B1M3-8.

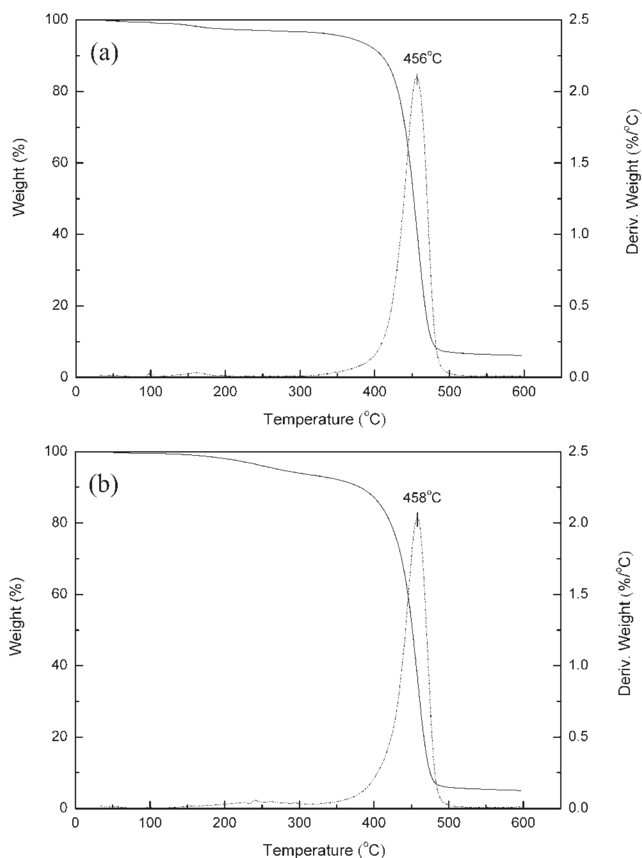

Figure 7 TGA and DTG thermograms of UV-cured (a) DPHA and (b) TMPTA.

a coupling agent (e.g., B1M0-8), the morphology of the formed photoresist underwent dramatic changes. As shown in Figure 6(b), some large domains (200–300 nm) emerged. This suggests that profound phase separation due to incompatibility between the silica and polymer matrix occurred in this sample. In contrast, when the coupling agent MSMA was employed (e.g., B1M3-8), large-scale phase separation no longer took effect. The micrograph shown in Figure 6(c) presents a dense and uniform morphology similar to that given in Figure 6(a). This is because MSMA possesses inorganic Si—OR groups that may form chemical bonds with Si—OH on the surface of SiO_2 particles in the sol. When that silica content was further increased to 21%, the formed photoresist still had very high uniformity, with a morphology similar to that shown in Figure 6(c).

Thermal properties

TGA

TGA was used to measure T_d of various samples. The TGA and differential thermogravimetry (DTG) thermograms of UV-cured DPHA and TMPTA are shown in Figure 7. These two crosslinked polymers exhibit similar degradation behavior with a maximum rate occurring close to 456°C. For poly(MMA/MAA)/SiO_2 and poly(MMA/MAA/MSMA)/SiO_2 series of photoresists, thermal decomposition follows a two-stage pattern. As an example, the TGA and DTG thermograms of the B1M0-x series are shown in Figure 8. For all cases, the first-stage decomposition occurred around 130–330°C, and the local maximum was at about 230°C [cf. Fig. 8(b)]. The main decomposition took place approximately over the range of 350–550°C. The weight loss in the first stage could be attributed to the intermolecular reaction of adjacent MMA and MAA monomer units, in which water and methanol were lost and anhydrides were produced, as pointed out by Mansur et al.[23] For the second-stage decomposition, two peaks can be identified. The lower temperature peak at about 420°C corresponds to the decomposition of MMA or MAA segments, whereas the higher peak accounts for the contribution from the crosslinking agent, TMPTA or DPHA (cf. Fig. 7). The content of the acrylate resin decreased with increasing SiO_2 content. For the

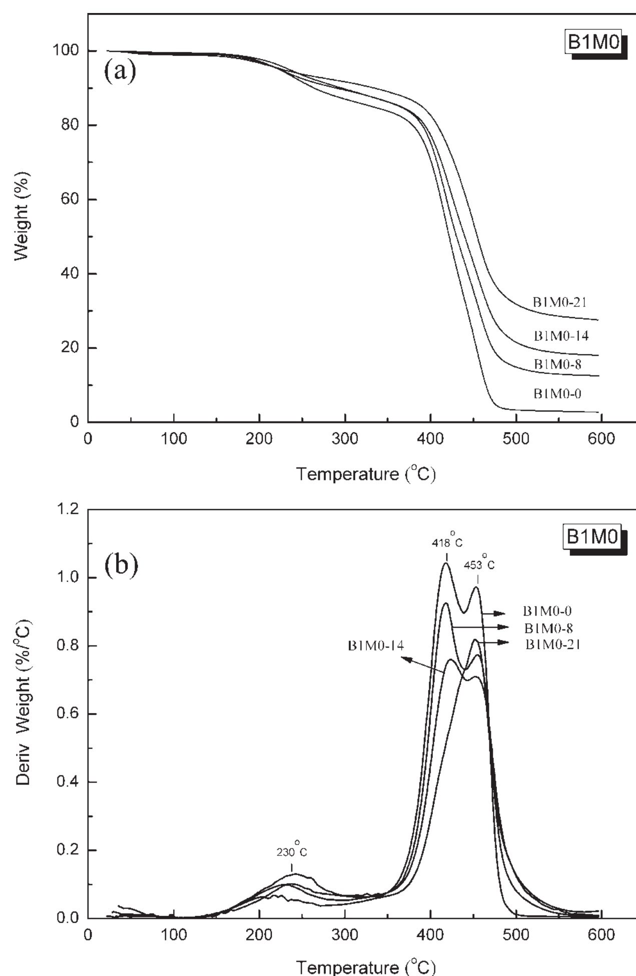

Figure 8 (a) TGA and (b) DTG thermograms of series B1M0-x.

TABLE II
T_d Values of Various Photoresists

Sample		$T_{d,\text{onset}}$ (°C)	Peak of derivative (°C)		Char yield (%)
			$T_{d,\max 1}$	$T_{d,\max 2}$	
B1M0-	0	374.8	417.5	453.5	2.8
	8	383.3	418.5	455.0	12.5
	14	386.5	422.0	452.0	18.0
	21	387.9	—	450.0	26.6
B1M1-	0	372.1	417.0	450.0	3.1
	8	375.5	423.0	450.0	14.2
	14	377.6	432.5	—	20.1
	21	384.7	427.0	449.0	25.7
B1M3-	0	376.9	417.0	454.0	3.5
	8	382.6	418.0	456.5	13.2
	14	384.4	421.0	455.0	18.2
	21	389.4	424.0	451.0	25.8
B1M5-	0	376.8	413.5	453.0	3.8
	8	382.3	423.0	450.5	14.1
	14	387.6	419.5	454.5	19.4
	21	394.6	—	450.0	26.3
B1M7-	0	383.6	413.0	453.5	3.9
	8	393.9	—	447.0	14.9
	14	395.9	—	448.0	20.6
	21	402.7	—	453.0	27.7

TABLE III
T_g Values of Photoresists from Thermal Analysis

Sample		T_g (°C)		
		DSC	DMA	TMA
B1M0-	0	117	—	117
	8	121	—	124
	14	129	—	131
	21	139	—	137
B1M1-	0	114	119	113
	8	122	124	122
	14	129	135	125
	21	141	141	132
B1M3-	0	115	119	116
	8	120	129	125
	14	—	135	129
	21	—	136	134
B1M5-	0	120	120	120
	8	—	123	126
	14	—	132	134
	21	—	134	132
B1M7-	0	119	121	118
	8	—	125	124
	14	—	131	131
	21	—	136	139

photoresist B1M0-21, the decomposition behavior at about 420°C was not that obvious because the SiO_2 content was raised up to 21 wt %. In fact, the same decomposition behavior was still observable, but it degenerated into a shoulder because of the increasing amount of SiO_2. Figure 8 also demonstrates the effect of silica. It can be seen that T_d increases with increasing silica content. In the extreme case, B1M0-21, the onset point of main thermal decomposition is about 13° higher than that of B1M0-0. For other series of photoresists, similar TGA behavior was observed, and the measured T_d values are given in Table II.

DMA

T_g values of various photoresists were measured with DMA, and the results are collected in Table III. Because samples in the B1M0 series were brittle, they broke easily on clamping to the sample holder, and hence their T_g could not be determined by DMA. For illustration, the thermograms of a typical series (B1M7) are shown in Figure 9. T_g was recognized as the temperature at the maximum value of the mechanical damping (tan δ). It appears that T_g of the samples increased with the increment of the SiO_2 content. The introduction of silica into the polymer matrix in the form of nanoparticles gave rise to a more rigid structure through extensive interfacial interactions between organic and inorganic phases. As the motions of the polymer chains were hindered extensively by nanosilica, T_g increased considerably. From Table III, it can be seen that an increase of 15–20°C could be achieved when the silica content reached 21% for various series of photoresists. Figure 9 also indicates that the tan δ peak faded gradually as the silica content was raised. For instance, the tan δ value was as small as 0.15, and the thermogram became relatively flat for sample B1M7-21. This means that the sample had a very low loss modulus with respect to the storage modulus; that is, it was low-damping and could store most energy in a damping cycle over the range of 50–180°C.

TMA

The linear thermal expansion coefficients of various photoresists were measured with TMA, and the

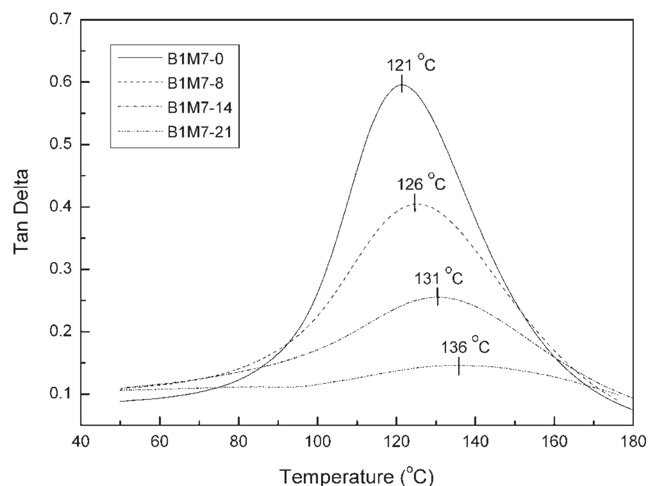

Figure 9 DMA thermograms of photoresists of the B1M7-*x* series.

TABLE IV
Coefficients of Thermal Expansion of Various Photoresists

Sample		α_1 (μm/m °C)	α_2 (μm/m °C)	T_g (°C)
B1M0-	0	175.2	365.8	117
	8	167.0	239.9	124
	14	162.4	181.1	131
	21	159.2	151.3	137
B1M1-	0	172.1	205.8	113
	8	164.6	184.1	122
	14	151.6	171.9	125
	21	154.7	158.3	132
B1M3-	0	160.0	216.6	116
	8	154.7	172.1	125
	14	147.0	162.3	129
	21	137.4	124.6	134
B1M5-	0	162.4	186.2	120
	8	164.5	171.8	126
	14	159.1	165.6	134
	21	147.3	157.0	132
B1M7-	0	153.6	191.1	118
	8	151.0	187.6	124
	14	150.2	163.7	131
	21	147.0	148.5	139

results are summarized in Table IV. Figure 10 shows the thermograms of a typical series of samples, B1M0-x, in terms of linear dimensional change versus temperature. For samples free of silica (B1M0-0), Figure 10 shows that α_2 and α_2 were 175 and 366 μm/m °C, respectively. T_g of this sample, as determined by the intersection of the two straight lines above and below the transition, was 117°C. The thermal expansion coefficients of polymers are normally very high, and this limits their industrial applications as coating materials. This shortcoming can be overcome by the incorporation of SiO_2 into the polymer host. From Figure 10, it can be seen that α_2 and α_2 of the formed photoresist films decreased with increasing silica content. Specifically, α_2 and α_2 of sample B1M0-21 were reduced to 159 and 151 μm/m °C, respectively. Measured data for other series of photoresists are collected in Table IV. It appears that the dimensional stability of the samples was improved by the addition of silica. The effect of MSMA on the thermal expansion coefficients was seen to be positive. According to the data listed in Table IV, when the comparison was based on the same silica content (e.g., B1Mx-8), all the photoresists containing MSMA had lower thermal expansion coefficients than the samples without MSMA (B1M0-8). It was also found that increasing the amount of MSMA to a certain value decreased both thermal expansion coefficients, α_1 and α_2. When the weight percentage of MSMA in the feed was 3 wt %, the synthesized photoresists, that is, B1M3-x, had the lowest thermal expansion coefficients. This agrees with the observation from the scanning electron microscopy (SEM) micrographs, which shows that 3 wt % MSMA could already reduce the level of phase separation to a nanoscale. A further increase in the MSMA amount did not further decrease the silica particle size. That means that there was an optimum amount of MSMA coupling agent added to the system. This could be attributed to the fact that MSMA was able to enhance the compatibility between the polymer and silica through chemical bonds. As silica was essentially incompressible, the extensive interfacial contact gave rise to the good dimensional stability of these samples.

DSC analysis

Attempts have been made to measure the T_g values of various series of samples by means of DSC. In Figure 11, the thermograms of the series B1M0 are shown. For samples B1M0-0 and B1M0-8, the glass-transition points are identified as 117 and 121°C,

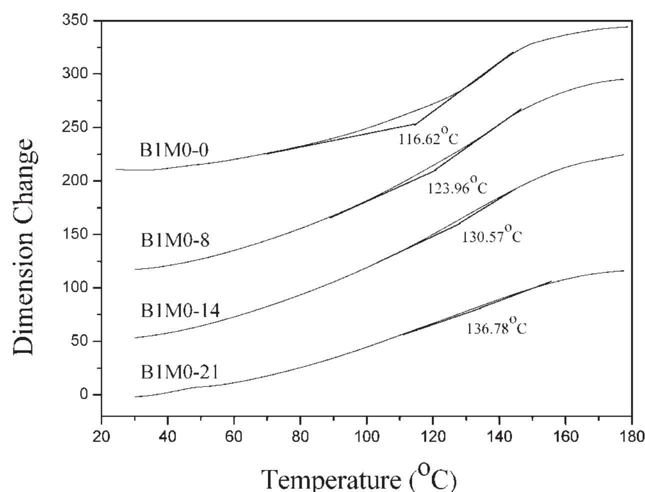

Figure 10 TMA thermograms of the B1M0-x series.

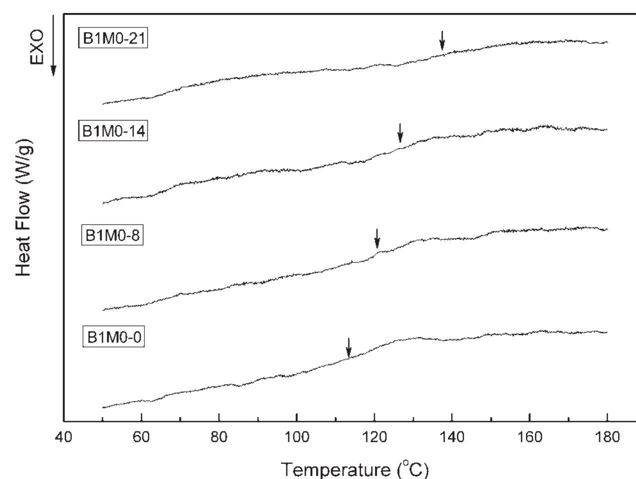

Figure 11 DSC thermograms of the B1M0-x series.

which are close to the results measured by TMA and given in Table IV. However, as the silica content was increased, the glass-transition phenomenon became unobvious from the thermogram. This is similar to DMA shown in Figure 9, in which the thermograms are relatively flat for high-silica-content samples. Other measurable T_g values are listed in Table III. They are similar to those determined by the DMA or TMA method. However, it is worthwhile to note that T_g values of various samples are not sensitive to the MSMA content, even though there is some small degree of increase between samples with and without MSMA, such as the B1M0-*x* and B1M1-*x* series. In fact, as shown previously, the level of phase separation could be reduced to a nanoscale by just a small dosage, such as 3% in Figure 6(c), of MSMA. Thus, T_g did not increase accordingly with a further increase in the MSMA content.

Generally, T_g values obtained with DMA are slightly higher than those of DSC or TMA. The difference in the T_g values is due to various factors, such as the heating rate, preparation of samples, operating conditions, and analytical methods. Even if the analytical methods are different, they all show the same trends in T_g values.

Adhesion, hardness, and resolution of the photoresists

The hardness of the cured photoresist coatings was examined with the industrial pencil test, whereas the adhesion strength of coatings on copper (deposited on printed circuit boards) was determined by the tape tests.[20] For all tested samples, the thickness of the dried coating layer was about 15 μm. All tested results are summarized in Table V. As expected, the hardness increased with increasing MSMA and SiO_2 contents. As for the adhesion tests, all photoresists showed perfect adhesion on the tape test, except sample B1M0-21, which contained 21% SiO_2 and was free of MSMA. It had very poor adhesion of 10%.

TABLE V
Hardness and Adhesion Measurements of Photoresists

		SiO_2 content (wt %)			
Sample	Property	0	8	14	21
B1M0	Hardness	2H	3H	3H	4H
	Adhesion	100	100	100	10
B1M1	Hardness	4H	4H	4H	4H
	Adhesion	100	100	100	100
B1M3	Hardness	4H	4H	4H	4H
	Adhesion	100	100	100	100
B1M5	Hardness	4H	4H	5H	5H
	Adhesion	100	100	100	100
B1M7	Hardness	5H	5H	5H	5H
	Adhesion	100	100	100	100

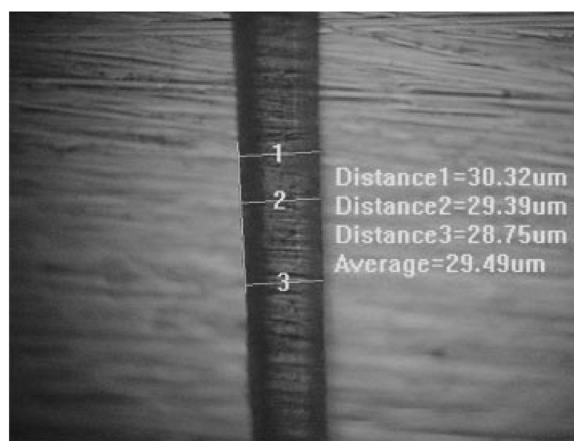

Figure 12 Optical microscopy image of a line in a circuit diagram showing the resolution of the photoresist.

This was associated with the fact that without MSMA, phase separation of this sample was serious. The large separated inorganic particles appeared to degrade the adhesion.

Finally, it is important to know how high a resolution the formed photoresist can achieve after a standard exposure-development process in case that practical industrial application is targeted. As an example, Figure 12 shows a microscopy image of a prepared photoresist, B1M7-21. The width of the line is about 30 μm, and the edge of the line is relatively flat and free of roughness. That is, the photoresist had a resolution meeting the industrial requirement.

CONCLUSIONS

In this research, a new type of negative photoresist was synthesized that consisted of silica nanoparticles dispersed uniformly in an MSMA-modified acrylic resin. The thermal and mechanical properties, morphology, and resolution of the formed photoresist were studied. Several points can be drawn from the experimental observations:

1. The coupling agent, MSMA, possessed inorganic functional groups that could form chemical bonds with silica particles, thereby enhancing the compatibility between the polymer and silica. With only a small dosage of MSMA, the size of the silica domain could be reduced significantly from several hundred nanometers to about 50 nm.
2. The incorporation of silica improved the thermal stability of the prepared photoresist: T_d and T_g were found to increase, whereas α_1 and α_2 decreased, with increasing silica content. MSMA also had a positive effect, and yet the improvement was moderate for T_d and the thermal expansion coefficient and low for T_g.

3. A photoresist coated on a copper substrate demonstrated high hardness (5H) and strong adhesion (100%), with a resolution reaching up to 30 μm.

References

1. Zhang, X.; Yang, J.; Zeng, Z.; Huang, L.; Chen, Y.; Wang, H.. Polym Int 2006, 55, 466.
2. Mager, M.; Schmalstieg, L.; Mechtel, M.; Kraus, H. Macromol Mater Eng 2001, 286, 682.
3. Lü, N.; Lü, X.; Jin, X.; Lü, C. Polym Int 2007, 56, 138.
4. Bauer, F.; Flyunt, R.; Czihal, K.; Buchmeiser, M. R.; Langguth, H.; Mehnert, R. Macromol Mater Eng 2006, 291, 493.
5. Wan, T.; Feng, F.; Rong, R.; Wang, Y. C. Polym Int 2006, 55, 883.
6. Chen, Y.; Zhou, S.; Yang, H.; Wu, L. Macromol Mater Eng 2005, 290, 1001.
7. Petrovic, Z. S.; Javni, I.; Waddon, A.; Banhegyi, G. J Appl Polym Sci 2000, 76, 133.
8. Zoppi, R. A.; Neves, S. D.; Nunes, S. P. Polymer 2000, 41, 5461.
9. Zhou, W.; Dong, J. H.; Qiu, K. Y.; Wei, Y. J Polym Sci Part A: Polym Chem 1998, 36, 1607.
10. Matejka, L.; Dukh, O.; Kolarik, J. Polymer 2000, 41, 1449.
11. Bosch, P.; Monte, F. D.; Mateo, J. L.; Levy, D. J Polym Sci Part A: Polym Chem 1996, 34, 3289.
12. Hajji, P.; David, L.; Gerard, J. F.; Pascault, J. P.; Vigier, G. J Polym Sci Part B: Polym Phys 1999, 37, 3172.
13. Pietrasik, J.; Zaborski, M. Polym Int 2005, 54, 1119.
14. Souza, F. L.; Bueno, P. R.; Longo, E.; Leite, E. R. Solid State Ionics 2004, 166, 83.
15. Wouters, M. E. L.; Wolfs, D. P.; van der Linde, M. C.; Hovens, J. H. P.; Tinnemans, A. H. A. Prog Org Coat 2004, 51, 312.
16. Soppera, O.; Croutxe-Barghorn, C.; Carre, C.; Blanc, D. Appl Surf Sci 2002, 186, 91.
17. Yu, Y. Y.; Chen, C. Y.; Chen, W. C. Polymer 2003, 44, 593.
18. Yu, Y. Y.; Chen, W. C. Mater Chem Phys 2003, 82, 388.
19. Hwang, S. T.; Hahn, Y. B.; Nahm, K. S.; Lee, Y. S. Colloids Surf A 2005, 259, 63.
20. Yu, S.; Wong, T. K. S.; Hu, X.; Wei, J. Microelectron Eng 2005, 77, 14.
21. Kim, H. K.; Kim, J. G.; Hong, J. W. Polym Test 2002, 21, 417.
22. Chen, W. C.; Lee, S. J. Polym J 2000, 32, 67.
23. Mansur, C. R. E.; Tavares, M. I. B.; Monteiro, E. E. C. J Appl Polym Sci 2000, 75, 495.